THE ASTROPHYSICAL JOURNAL, 464:L115–L118, 1996 June 20
© 1996. The American Astronomical Society. All rights reserved. Printed in U.S.A.

MAXIMUM LIKELIHOOD CLUSTER RECONSTRUCTION

MATTHIAS BARTELMANN,[1,2] RAMESH NARAYAN,[2] STELLA SEITZ,[1] AND PETER SCHNEIDER[1]
Received 1995 September 8; accepted 1996 January 11

ABSTRACT

We present a novel method to reconstruct the mass distribution of galaxy clusters from their gravitational lens effect on background galaxies. The method is based on a least-χ^2 fit of the two-dimensional gravitational cluster potential. The method combines information from shear and magnification by the cluster lens and is designed to easily incorporate possible additional information. We describe the technique and demonstrate its feasibility with simulated data. Both the cluster morphology and the total cluster mass are well reproduced.

Subject headings: galaxies: clusters: general — gravitational lensing — methods: numerical

1. INTRODUCTION

It is of considerable interest for cosmology and the theory of structure formation in the universe to learn about the amount and the spatial distribution of mass in galaxy clusters. While other methods to determine cluster masses depend on restrictive assumptions about the symmetry and the equilibrium of the clusters, gravitational lensing is sensitive to the entire gravitating mass of the lens, regardless of its composition and its dynamical state. The drawback of lensing-based methods is that they determine the projected mass, thus giving rise to ambiguities from projection effects; however, these methods should be compared with the uncertainties of X-ray and dynamical mass estimates.

Attempts to determine cluster mass distributions from lensing date back to the suggestion by Webster (1985) that clusters might act as efficient lenses on background populations of extended objects, and to the detection of a coherent shear pattern in the field of the cluster Abell 1689 by Tyson, Valdes, & Wenk (1990). Kochanek (1990) and Miralda-Escudé (1991) discussed how parameterized cluster mass distributions could be constrained from observations of weak lensing in cluster fields. A technique for parameter-free cluster inversion was pioneered by Kaiser & Squires (1993), who found that the surface mass density of galaxy clusters can be derived in terms of a convolution of the observed shear pattern with a kernel describing the shear of a point mass. The feasibility of this and related approaches was then demonstrated by a number of authors (e.g., Bonnet, Mellier, & Fort 1994; Fahlman et al. 1994; Smail et al. 1995; Tyson & Fischer 1995), and Kaiser, Squires, & Broadhurst (1995) and Bonnet & Mellier (1995) described techniques to determine galaxy shapes accurately from observed cluster fields.

The cluster inversion technique as proposed by Kaiser & Squires (1993) is designed for weak cluster lenses, and it causes unwanted boundary effects in small or irregularly shaped cluster fields. Schneider & Seitz (1995), Seitz & Schneider (1995), and Kaiser (1995) extended the method into the nonlinear regime, and Schneider (1995), Kaiser et al. (1995b), Bartelmann (1995), and Seitz & Schneider (1996) described how the boundary effects can be removed.

All cluster reconstruction techniques based on image distortions alone can determine the cluster mass distribution only up to a one-parameter family of linear transformations. This so called mass-sheet degeneracy was originally found by Gorenstein, Falco, & Shapiro (1988) and discussed in the context of cluster lensing in the weak limit by Kaiser & Squires (1993), and generally by Schneider & Seitz (1995). The degeneracy can be broken if information on the image magnification is employed, as suggested by Broadhurst, Taylor, & Peacock (1995) and Bartelmann & Narayan (1995).

Unambiguous determinations of cluster masses from weak lensing require the redshift distribution of background sources to be known. Apart from direct spectroscopy, which is hampered by the faintness of the background sources, lensing itself provides the means to find faint-galaxy redshifts. Kneib et al. (1994) estimated arclet redshifts in the field of the cluster Abell 370, and Smail, Ellis, & Fitchett (1994) discussed how faint-galaxy redshifts can be constrained from weak lensing by a number of clusters. Bartelmann & Narayan (1995) proposed an algorithm to simultaneously derive cluster mass distributions and the redshift distribution of faint galaxies.

Here we propose a novel cluster-reconstruction technique that is local, thus avoiding boundary effects by design, and that combines information on galaxy distortions and magnifications, thus breaking the mass-sheet degeneracy. The key idea is to reconstruct the two-dimensional Newtonian potential of the cluster lenses with a least-χ^2 approach. The least-χ^2 method lends itself to straightforwardly including additional information into the cluster-reconstruction process. We aim at the gravitational potential rather than at the surface mass density because it is the physical object underlying both lensing distortion and magnification, and because it should simplify comparisons of determinations of the cluster mass distribution from gravitational lensing with those from other means—e.g., interpretations of the X-ray emission.

This Letter outlines the method and demonstrates its feasibility using simulated data. Extensions and a detailed discussion are postponed to a later, more technical paper (Seitz et al. 1996). Section 2 describes the technique. In § 3, we present results from numerical simulations, and we summarize the Letter in § 4.

[1] Max-Planck-Institut für Astrophysik, Karl-Schwarzschild-Straße 1, D-85748 Garching, Germany.
[2] Harvard-Smithsonian Center for Astrophysics, 60 Garden Street, Cambridge MA 02138.

2. OUTLINE OF THE METHOD

Gravitational lensing magnifies and distorts images of extended background sources. The local properties of the lens mapping are described by the Jacobian

$$\mathcal{A} = \frac{\partial \boldsymbol{y}}{\partial \boldsymbol{x}} = \begin{pmatrix} 1 - \kappa - \gamma_1 & -\gamma_2 \\ -\gamma_2 & 1 - \kappa + \gamma_1 \end{pmatrix}, \tag{1}$$

where $\boldsymbol{x}$ and $\boldsymbol{y}$ are dimensionless, two-dimensional position vectors in the lens and source planes, respectively. The convergence κ is the scaled surface mass density of the lens, and $\gamma_{1,2}$ are the components of the shear. They are combinations of second derivatives of the (dimensionless) two-dimensional Newtonian potential of the lens,

$$\kappa = \tfrac{1}{2}(\psi_{,11} + \psi_{,22}), \quad \gamma_1 = \tfrac{1}{2}(\psi_{,11} - \psi_{,22}), \quad \gamma_2 = \psi_{,12}. \tag{2}$$

For general reference on lensing, see Schneider, Ehlers, & Falco (1992) or Blandford & Narayan (1992). Image distortions, which can be quantified by, e.g., the quadrupole tensor of the surface brightness distribution, measure the two-component quantity

$$g_i = \frac{\gamma_i}{1 - \kappa} \tag{3}$$

(Miralda-Escudé 1991; Schneider 1995; Kaiser 1995). Since the ellipticity of an image is independent of its size, the ellipticity is unchanged if the Jacobian is multiplied by a factor $\lambda \neq 0$, which corresponds to transforming κ and γ_i according to

$$(1 - \kappa) \to \lambda(1 - \kappa), \quad \gamma_i \to \lambda\gamma_i. \tag{4}$$

The lens strength g_i (above) is manifestly invariant under this transformation, which reflects the mass-sheet degeneracy mentioned in the introduction. If the cluster has a critical curve, an ambiguity arises in the g_i because of the parity change upon crossing the critical curve. An unambiguous measure of the ellipticity is then provided by the distortion δ_i,

$$\delta_i = \frac{2\gamma_i(1 - \kappa)}{(1 - \kappa)^2 + \gamma_1^2 + \gamma_2^2}$$

(Schneider & Seitz 1995; Miralda-Escudé 1991).

The magnification μ is given by

$$\mu = \det{}^{-1}\mathcal{A} = [(1 - \kappa)^2 - \gamma_1^2 - \gamma_2^2]^{-1}, \tag{5}$$

which scales with λ^{-2} under the transformation in equation (4). Measurements of the magnification can therefore be used to break the mass-sheet degeneracy, as Broadhurst et al. (1995) recognized. The magnification is accessible on a statistical basis by comparing the sizes of galaxies in cluster fields with those of galaxies of equal surface brightness in empty fields, or by the change in number density of galaxies (Bartelmann & Narayan 1995; Broadhurst et al. 1995).

In the following, we assume that the sizes and shapes of galaxies in a cluster field and in an empty control field have been determined. The data are averaged over suitable regions of the cluster field to reduce the noise. These regions have to be small enough so that the properties of the lens can be assumed to be constant across each region, and large enough so that they contain a sufficient number of galaxies. Since the number of background galaxies is of the order of 10^5 per square degree at $B \approx 27$ (e.g., Tyson 1994), this requirement is easily met. We do the smoothing with a Gaussian filter. The smoothing length is spatially constant and is varied later to minimize the χ^2 obtained in the fit.

For simplicity, we assume in the following that we already have the smoothed data on a regular grid covering the cluster field; i.e., that we have obtained smoothed measurements $g_i(k, l)$ and $\mu(k, l)$ of the two components of the lens strength and the magnification in each cell (k, l) of the grid. For simplicity of notation, we use the inverse magnification $r(k, l) \equiv \mu^{-1}(k, l)$ rather than the magnification.

Of course, local estimates of the surface-mass density can be obtained directly, once g and r are given at each grid cell (Broadhurst 1996). However, such an approach has the major disadvantage that it neglects the fact that convergence and shear are intrinsically related fields. This relation provides important additional information, and thus considerably reduces the noise of the reconstruction. In our approach, the one physical field ψ underlying all local lensing effects is reconstructed, and it is determined in such a way as to optimize the global agreement of ψ with the data.

We now want to determine least-χ^2 fits to the values of the potential $\psi(k, l)$ in the cells (k, l) of the data grid. To do so, we replace the second partial derivatives of the potential in equation (2) by their second-order, finite-difference approximations. The resulting expressions can then be used to form estimators $\hat{g}_i(k, l)$ and $\hat{r}(k, l)$, in terms of ψ for the lens strength $g_i(k, l)$ and the inverse magnification $r(k, l)$ at the grid cell (k, l). The appropriate χ^2 function then reads

$$\chi^2 = \sum_{k,l} \left\{ \frac{1}{\sigma_g^2(k, l)} [g_i(k, l) - \boldsymbol{g}_i(k, l)]^2 + \frac{1}{\sigma_r^2(k, l)} [r(k, l) - \boldsymbol{r}(k, l)]^2 \right\}, \tag{6}$$

where summation over the two components of g_i is implied. Of course, χ^2 depends on the values $\psi(m, n)$ of the potential at the grid points (m, n). The variances $\sigma_g(k, l)$ and $\sigma_r(k, l)$ of g and r can be estimated directly from the data. Since the derivatives

$$\frac{\partial \chi^2}{\partial \psi(m, n)}$$

are straightforwardly determined, χ^2 can then be minimized numerically using a conjugate-gradient algorithm (e.g., Press et al. 1992, § 10.6).

It is implicitly assumed in equation (6) that g and r can be determined independently, which is the case in our simulation. In practice, however, g and r can be correlated especially for faint images. In that case, one would determine the local averages of g and r by giving lesser weight to fainter images, and modify the definition of χ^2 in such a way as to account for a possible correlation.

The grid for the potential coincides with the grid of the smoothed data within the observed field, but it has to be extended by one further row or column of grid cells along each side of the field to allow the partial derivatives to be determined at any grid point where data are given. We start the potential fit with $\psi(m, n) = 0$ for all (m, n). Since only second derivatives of the potential enter into the algorithm, we are

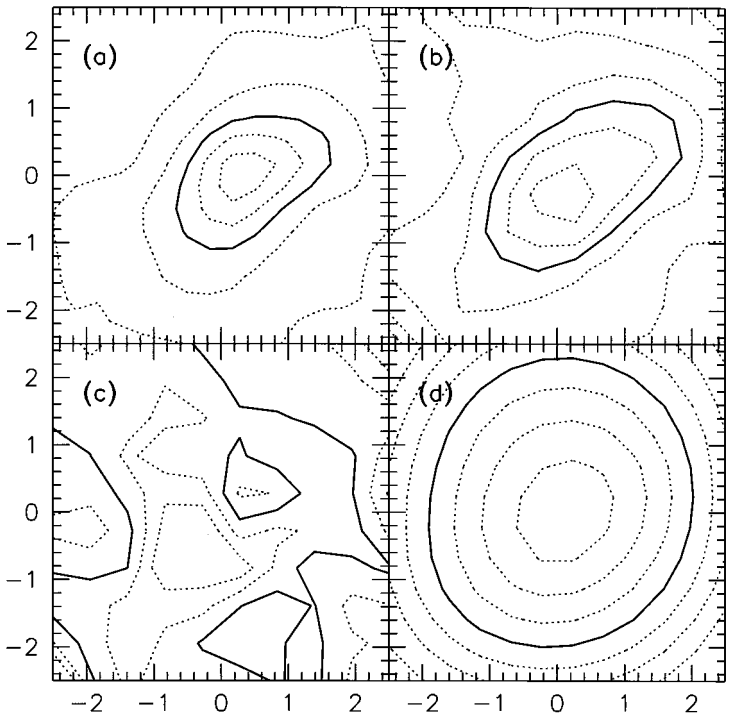

FIG. 1.—Four contour plots showing (*a*) the original cluster model, (*b*) the reconstruction, (*c*) the difference between the two, and (*d*) the dimensionless, two-dimensional potential. Contours in (*a*) and (*b*) are spaced by 0.1, and the heavy contour follows $\kappa = 0.5$. In (*c*), contours are spaced by 0.05 and the heavy contour follows $\Delta\kappa = 0$. The potential is kept fixed at $\psi = 0$ at three corners. The heavy line in (*d*) follows the arbitrary contour $\psi = -5$, and the contours are spaced by 1.5. The side length of the fields is 5′.

free to add an arbitrary constant and a spatially constant gradient to the potential. We choose to fix the potential to $\psi = 0$ at three corners of the field. The result is a least-χ^2 fit of the potential values $\psi(m, n)$ on the grid, from which κ and thus the surface mass density can be derived via equation (2). In short, the χ^2 minimization determines the potential in such a way as to optimize the agreement between the measured ellipticities and sizes of the lensed galaxies, and the shear and the convergence expected from the potential.

3. NUMERICAL SIMULATIONS

For testing the method, we use a numerically simulated galaxy cluster from the sample described in detail by Bartelmann, Steinmetz, & Weiss (1995). Briefly, the cluster was simulated within a *COBE*-normalized CDM cosmological simulation, taking the tidal forces of the surrounding structures into account. The cluster model we select is at redshift $z_d = 0.16$. It is resolved into ~17,000 particles, whose line-of-sight velocity dispersion is ~1200 km s^{-1}.

Background galaxies are assumed to be at a constant redshift of $z_s = 1$. They are assigned random intrinsic ellipticity components (ϵ_1, ϵ_2) drawn from the probability distribution

$$p_e(\epsilon_1, \epsilon_2) = \frac{\exp\left(-|\epsilon|^2/\sigma_\epsilon^2\right)}{\pi\sigma_\epsilon^2[1 - \exp\left(-1/\sigma_\epsilon^2\right)]}, \qquad (7)$$

where $|\epsilon|^2 \equiv \epsilon_1^2 + \epsilon_2^2$. For elliptical images, the modulus of ϵ is given by

$$|\epsilon| = \frac{a - b}{a + b},$$

where a and b are the major and minor axes of the ellipse, respectively. We choose $\sigma_\epsilon = 0.15$ (cf. Miralda-Escudé 1991; Tyson & Seitzer 1988; Brainerd, Blandford, & Smail 1995). Further galaxy properties are chosen according to the galaxy model motivated and described by Bartelmann & Narayan (1995). They include luminosity and surface brightness, which allow us to assign an intrinsic size to the sources. The logarithmic variance of the intrinsic galaxy radii is $\Delta\ln R \approx 0.5$, in good agreement with *HST* measurements (N. Kaiser 1994, private communication).

We simulate the lensing effect of the cluster on the sources, assuming a source density of 70 galaxies per square arcminute. In addition, we simulate an independent empty galaxy field to calibrate the intrinsic sizes of the sources needed for our algorithm. The field side length is 5′, and the field is covered by a grid of 10×10 cells (or 12×12 cells for the potential). The simulated galaxy data in the lensed and the unlensed fields are then analyzed with the least-χ^2 potential reconstruction method described previously. We vary the smoothing length in such a way as to minimize the χ^2 obtained by the potential fit. Various results are presented in Figures 1 and 2 The χ^2 per degree of freedom in this case is 1.08, with about equal contributions from the distortion and the size information.

Figure 1 shows contour plots of the original cluster model in panel *a*, the reconstruction in panel *b*, the difference between these two in panel *c*, and the potential in panel *d*. A comparison between the upper panels shows that the cluster is very well reproduced, except that the involved smoothing of the data tends to broaden the central mass peak. The agreement is quantified in panel *c*, which shows that the residual is small and distributed fairly homogeneously across the field. In

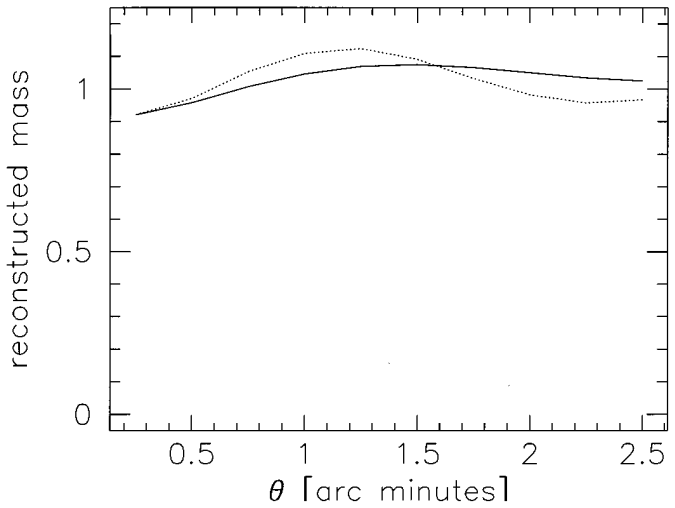

FIG. 2.—Reconstructed mass fraction within circles centered on the cluster center. The solid curve shows the fraction of the cumulative mass within radius θ, the dotted curve shows the mass fraction within annuli, and θ is given in arcminutes.

particular, there are no systematic deviations toward the field boundary.

Figure 2 displays two curves. The solid curve shows the total mass within radius θ from the center of the cluster, relative to the input mass, i.e., the cumulative mass fraction within circles as a function of the circle radius. The dotted curve shows the mass fraction in annuli with outer radius θ and width $0'.25$. The solid curve starts at ~ 0.92, rises to ~ 1.07, and falls toward ~ 1 at the field boundary. This shows that the total cluster mass enclosed by circles is reproduced to $\sim 7\%$ at any radius, and to higher accuracy at the field boundary. The mass fraction in annuli shows a somewhat larger fluctuation of $\sim \pm 10\%$. Both curves underestimate the mass in the cluster center because the smoothing involved in the preparation of the input data tends to broaden the central mass peak, thereby shifting mass to larger radii. This local overestimate at intermediate radii is compensated by a slight underestimate at larger radii such as to reproduce the total mass, which is fixed by the overall magnification effect of the cluster.

4. SUMMARY

We have suggested a novel method to reconstruct cluster mass distributions from their gravitational lens effect on a population of background sources. Both distortion and magnification effects are included. The method is based on a least-χ^2 fit of the two-dimensional Newtonian potential of the lensing cluster. Reconstructing the potential is advantageous because it is the physical quantity underlying both the distortion and the magnification. The least-χ^2 approach has the advantages that it provides a local reconstruction technique, which renders it insensitive to boundary effects, and that it can be almost arbitrarily extended to incorporate additional information. The combination of shear and magnification effects breaks the mass-sheet degeneracy inherent in all reconstruction algorithms based on ellipticity information alone.

Application of our method requires the measurement of not only the ellipticities of background galaxies but also their intrinsic and their magnified sizes. Although the intrinsic dispersion of the sizes is large, the large number density of background galaxies supplies a sufficiently large database to statistically extract reliable information on the magnification. The intrinsic sizes of the background galaxies are to be obtained from observations in empty fields.

Using numerical simulations, we have demonstrated that the method accurately reproduces the shape and the total mass in the lensing cluster. The lensing cluster was numerically simulated within a CDM scenario, taking the tidal field of the surrounding matter distribution into account. The numerically simulated population of background galaxies was adapted to observations; it is designed to reproduce the observed intrinsic scatter in galaxy sizes and ellipticities, and the number density of these objects.

Various modifications and refinements are possible and can be included in the proposed technique. Among them are the effect of the lensing magnification on the number density of background galaxies (originally discussed by Broadhurst et al. 1995), and regularized maximum likelihood techniques to avoid the (to some degree arbitrary) smoothing of the data and to ensure that the fitted data points are independent. Such modifications and extensions will be discussed in a following paper (Seitz et al. 1996).

We thank Bill Press for valuable comments and Matthias Steinmetz for the numerical simulation of the cluster model. This work was partially supported by the Sonderforschungsbereich SFB 375-95 of the Deutsche Forschungsgemeinschaft (M. B., S. S., P. S.), and by NSF grants AST 9423209 and PHY 94-07194 (R. N.).

REFERENCES

Bartelmann, M. 1995, A&A, 303, 643
Bartelmann, M., & Narayan, R. 1995, ApJ, 451, 60
Bartelmann, M., Steinmetz, M., & Weiss, A. 1995, A&A, 297, 1
Blandford, R. D., & Narayan, R. 1992, ARA&A, 30, 311
Bonnet, H., & Mellier, Y. 1995, A&A, 303, 331
Bonnet, H., Mellier, Y., & Fort, B. 1994, ApJ, 427, L83
Brainerd, T. G., Blandford, R. D., & Smail, I. 1995, preprint
Broadhurst, T. J. 1996, ApJ, submitted
Broadhurst, T. J., Taylor, A. N., & Peacock, J. A. 1995, ApJ, 438, 49
Fahlman, G., Kaiser, N., Squires, G., & Woods, D. 1994, ApJ, 437, 56
Gorenstein, M. V., Falco, E. E., & Shapiro, I. I. 1988, ApJ, 327, 693
Kaiser, N. 1995, ApJ, 493, L1
Kaiser, N., & Squires, G. 1993, ApJ, 404, 441
Kaiser, N., Squires, G., & Broadhurst, T. J. 1995a, ApJ, 449, 460
Kaiser, N., Squires, G., Fahlman, G., Woods, D., & Broadhurst, T. 1995b, in press
Kneib, J.-P., Mathez, G., Fort, B., Mellier, Y., Soucail, G., & Longaretti, P.-Y. 1994, A&A, 286, 701
Kochanek, C. S. 1990, MNRAS, 247, 135
Miralda-Escudé, J. 1991, ApJ, 370, 1
Press, W. H., Teukolsky, S. A., Vetterling, W. T., & Flannery, B. P. 1992, Numerical Recipes (Cambridge: Cambridge Univ. Press)
Schneider, P., 1995, A&A, 302, 639
Schneider, P., Ehlers, J., & Falco, E. E. 1992, Gravitational Lenses (Heidelberg: Springer)
Schneider, P., & Seitz, C. 1995, A&A, 294, 411
Seitz, C., & Schneider, P. 1995, A&A, 297, 287
Seitz, S., & Schneider, P. 1996, A&A, 305, 383
Seitz, S., Schneider, P., Bartelmann, M., & Narayan, R. 1996, in preparation
Smail, I., Ellis, R. S., & Fitchett, M. J. 1994, MNRAS, 270, 245
Smail, I., Ellis, R. S., Fitchett, M. J., & Edge, A. C. 1995, MNRAS, 273, 277
Tyson, J. A. 1994, in Proc. Les Houches Summer School, Cosmology and Large-Scale Structure, ed. R. Schaeffer et al. in press
Tyson, J. A., & Fischer, P. 1995, ApJ, 446, L55
Tyson, J. A., & Seitzer, P. 1988, ApJ, 335, 552
Tyson, J. A., Valdes, F., & Wenk, R. A. 1990, ApJ, 349, L1
Webster, R. L. 1985, MNRAS, 213, 871